THE GREAT WORLD OF NANOTECHNOLOGY

Marcos Augusto de Lima Nobre

(Organizador)

VOL II

EDITORA ARTEMIS

2021

THE GREAT WORLD OF NANOTECHNOLOGY

Marcos Augusto de Lima Nobre

(Organizador)

VOL II

EDITORA ARTEMIS

2021

Editora Chefe	Profª Drª Antonella Carvalho de Oliveira
Editora Executiva	M.ª Viviane Carvalho Mocellin
Direção de Arte	M.ª Bruna Bejarano
Diagramação	Elisangela Abreu
Organizadoras	Prof. Dr. Marcos Augusto de Lima Nobre
Imagem da Capa	Kateryna Kon
Bibliotecário	Maurício Amormino Júnior – CRB6/2422

Editora Artemis
Curitiba-PR Brasil
www.editoraartemis.com.br
e-mail:publicar@editoraartemis.com.br

Dados Internacionais de Catalogação na Publicação (CIP)
(eDOC BRASIL, Belo Horizonte/MG)

G786 The great world of nanotechnology [livro eletrônico] : vol. II / Organizador Marcos Augusto de Lima Nobre. – Curitiba, PR: Artemis, 2021.

Formato: PDF
Requisitos de sistema: Adobe Acrobat Reader
Modo de acesso: World Wide Web
Inclui bibliografia
Edição bilíngue
ISBN 978-65-87396-36-1
DOI 10.37572/EdArt_300621361

1. Nanociência. 2. Nanotecnologia. I. Nobre, Marcos Augusto Lima.

CDD 620.5

Elaborado por Maurício Amormino Júnior – CRB6/2422

EDITORA ARTEMIS
2021

Editora Artemis
Curitiba-PR Brasil
www.editoraartemis.com.br
e-mail:publicar@editoraartemis.com.br

PREFACE

The insertion of new and enhanced materials based on materials belonging to the Nano scale in the day-by-day has growth up in a silent way. In part, a number of works in the nanotechnology stemming of theoretical research using Density Functional Theory (DFT) and sophisticated simulation methods; another part is associated to the protected technologies associated to the military and patented nanomaterial and its process. In this sense, open access to recent aspects on the nanostructures application and properties can be reached in this book. Here, an interesting set of chapters gives opportunity of access texts that reach process and processing of nanostructures, applications of nanotechnology, advanced techniques to theoretical development. A broad set of nanostructures are here covered such as, nanocrystal, superficial nanograins, inner microstructures with nanograins, nanoaggregates, nanoshells, nanotubes, nanoflowers, nanoroad, nanosheets, Also, reveals new investigations areas as grainboundary of nanograins in ceramics and metals. A great number of software has been used as a tool of development of Science and Technologies for nanotechnology COMSOL Multiphysics 5.2. Phenomena and properties has been investigated by recent or classical techniques of materials characterization as Localized Surface Plasmon Resonance (LSPR), X-ray photoelectron spectroscopy (XPS), Field Emission Gun Scanning Electron Microscopy (FEG-SEM) with Energy Dispersive Spectroscopy (EDS), Raman Scattering Spectroscopy (RSS), X ray diffraction (XRD), ^{57}Fe Mössbauer spectroscopy, UV-vis spectroscopy, dynamic light scattering (DLS), Atomic Force Microscopy (AFM), and Field Emission Gun Scanning Electron Microscopy (FEG-SEM). In this sense, collections of spectra from Mössbauer spectroscopy, UV-vis spectroscopy and Infrared spectroscopy can be found. As a matter of fact, some chapter's item can be seemed as specific protocols for synthesis, preparations and measurements in the nanotechnology.

I hope you enjoy your reading.

Prof. Dr. Marcos Augusto Lima Nobre

TABLE OF CONTENTS

CHAPTER 1 1

ROLLING OF 316L STAINLESS STEEL WITH ROUGH ROLLS: A POSSIBLE TECHNIQUE TO OBTAIN SUPERFICIAL NANOGRAINS

Carlos Camurri
Alejo Gallegos

DOI 10.37572/EdArt_3006213611

CHAPTER 2 11

EFFECTS OF DIFFERENT ASPECT RATIOS AND JUNCTION LENGTHS ON THE COUPLED PLASMON GOLD NANOROD DIMERS

Hafiz Zeeshan Mahmood
Umer Farooq
Usman Rasool
Noor ul Huda
Sana Gulzar
Mahmood Ali
Maryam Iftikhar
Yasir Javed
Sajid Farooq

DOI 10.37572/EdArt_3006213612

CHAPTER 3 21

AB-INITIO STUDY OF ELECTRONIC AND MAGNETIC PROPERTIES OF ZnO NANOCRYSTALS CAPPED WITH ORGANIC MOLECULES

Aline L. Schoenhalz
Paulo Piquini

DOI 10.37572/EdArt_3006213613

CHAPTER 4 39

CONFINED WATER CHEMISTRY: THE CASE OF NANOCHANNELS GOLD OXIDATION

André Mourão Batista
Herculano da Silva Martinho

DOI 10.37572/EdArt_3006213614

CHAPTER 5 .... **67**

PLASMONIC RESPONSE OF GOLD- SILICA AND SILVER- SILICA METAL CORE NANOSHELLS BY OPTIMIZING THE FIGURE OF MERIT

Hafiz Zeeshan Mahmood
Zainab Shahid
Alina Talat
Imama Irfan
Bushra Arif
Sana Habib
Saba Munawar
Yasir Javed
Shaukat Ali Shahid
Sajid Farooq

DOI 10.37572/EdArt_3006213615

CHAPTER 6 .... **76**

AMORPHOUS MICRO AND NANO SILICA EXTRACTED FROM RICE HUSKS AND OBTAINED BY ACIDIC PREHYDROLYSIS AND CALCINATION: PREPARATION ROUTE AND CHARACTERIZATION

Eduardo Roque Budemberg
Elton Aparecido Prado dos Reis
Deuber Lincon da Silva Agostini
Renivaldo José dos Santos
Felipe Silva Bellucci
Aldo Eloizo Job
Daltro Garcia Pinatti
Rosa Ana Conte

DOI 10.37572/EdArt_3006213616

CHAPTER 7 .... **92**

FORMATION OF METAL NANOPARTICLES BY SPUTTER DEPOSITION ON UNCD FILMS BY NPIII INSIDE CONDUCTIVE TUBES

Nazir Monteiro dos Santos
Divani Carvalho Barbosa
Evaldo José Corat
Mario Ueda

DOI 10.37572/EdArt_3006213617

CHAPTER 8 .... **109**

X-RAY PHOTOELECTRON SPECTROSCOPY (XPS) STUDY OF CONDUCTIVE TUBE AFTER NITROGEN PIII

Nazir Monteiro dos Santos
Elver Juan de Dios Mitma Pillaca
Mario Ueda
Steven Frederick Durrant
Pericles Lopes Sant'Ana

DOI 10.37572/EdArt_3006213618

CHAPTER 9 .... **125**

APPLICATION OF CLAY-CARBOXIMETHYLCHITOSANE NANOCOMPOSITE-SILVER NANOPARTICLES IN FILTERS TO TREAT CONSUMPTION WATER IN RURAL AREAS OF CAMANA - AREQUIPA-PERU

Maria Elena Talavera Nuñez
Irene Zea Apaza
Corina Vera Gonzales
Julia Zea Alvarez
Luis Rodrigo Benavente Talavera

DOI 10.37572/EdArt_3006213619

CHAPTER 10 .... **138**

NANOGRAIN BOUNDARY PHENOMENON IN CERAMIC NANOMETRIC MICROSTRUCTURE

Marcos Augusto Lima Nobre
Silvania Lanfredi

DOI 10.37572/EdArt_30062136110

CHAPTER 11 .... **150**

ON SPIN HAMILTONIAN FITS TO MÖSSBAUER SPECTRA OF NIFE2O4 NANOPARTICLES SYNTHESIZED BY CO-PRECIPITATION

Jose Higino Dias Filho
Jorge Luis Lopez
Adriana Silva de Albuquerque
Renato Dourado Maia
Wesley de Oliveira Barbosa
Ernando Campos Ferreira
Fellipe Silva Pereira
Kátia Guimarães Benfica

DOI 10.37572/EdArt_30062136111

CHAPTER 12 .... **162**

EFFECT OF GRAPHITE NANOSTRUTURES ON THE VISCOSITY PROPERTIES OF BLENDS DIESEL-S10 AND BIODIESEL

Túlio Begena Araújo
Marcos Augusto Lima Nobre

DOI 10.37572/EdArt_30062136112

CHAPTER 13 .... **172**

REMOCIÓN DE ARSÉNICO DE EFLUENTES ACUOSOS EMPLEANDO COMO ADSORBENTE MAGNETITA NANOESTRUCTURADA

Orfelinda Avalo Cortez
Luis Jean Carlo Cisneros García
David Pedro Martínez Aguilar

DOI 10.37572/EdArt_30062136113

CHAPTER 14 .... **182**

AVALIAÇÃO DA MICRODUREZA DE NANOCOMPÓSITOS DE MATRIZ DE ALUMÍNIO REFORÇADOS COM ÓXIDO DE GRAFENO REDUZIDO

Daniel Andrada Maria
Andreza de Sousa Andrada Jordânio
Samuel Siqueira
Adelina Pinheiro Santos
Clascídia Aparecida Furtado

DOI 10.37572/EdArt_30062136114

CHAPTER 15 .... **197**

ROTA ECOLOGIA PARA SINTESE DE ELETRODO NANOESTRUTURADO DE ZnO PARA SUPERCAPACITOR

Eguiberto Galego
Marilene Morelli Serna
Tatiane Yumi Tatei
Bruna Rodrigues de Lima
Rubens Nunes de Faria Junior

DOI 10.37572/EdArt_30062136115

CHAPTER 16 .... **212**

MORFOLOGIA DE FILMES FINOS NANOESTRUTURADOS DE ZnO PRODUZIDOS PELO MÉTODO SILAR

Eguiberto Galego
Marilene Morelli Serna
Lalgudi Venkataraman Ramanathan
Rubens Nunes de Faria Junior

DOI 10.37572/EdArt_30062136116

CHAPTER 17 .... **228**

OBTENÇÃO E CARACTERIZAÇÃO DE NANOCRISTAIS DE CELULOSE A PARTIR DE PAPEL RECICLADO VIRGEM E PÓS-CONSUMO

Jean Brito Santos
Emanoel Igor da Silva Oliveira
Nádia Mamede José

DOI 10.37572/EdArt_30062136117

ABOUT THE ORGANIZER **234**

INDEX **236**

CHAPTER 1

ROLLING OF 316L STAINLESS STEEL WITH ROUGH ROLLS: A POSSIBLE TECHNIQUE TO OBTAIN SUPERFICIAL NANOGRAINS

Data de submissão: 17/03/2021
Data de aceite: 06/04/2021

Carlos Camurri
University of Concepción
Department of Materials Engineering
Concepción, Chile

Alejo Gallegos
University of Concepción
Department of Materials Engineering
Concepción, Chile

ABSTRACT: 316L stainless steel plates of 5 mm thickness, normalized at 900°C, were cold rolled with different reductions and number of passes by using rolls with three different surface roughnesses: grain heights of 0.17 and 0.33 mm and rombhoid-shaped grains of 1.5 mm height. Subsequently, the rolled samples were annealed at 275°C for 1 h in an effort to achieve superficial nanograins. The plates laminated by using low-roughness rolls had continuous superficial microcrystallization when they were rolled for at least 26 passes. For samples made with rougher rolls, the recrystallized superficial grains formed on the surface (sized ~10–15 μm) were smaller than those below the surface; this behavior was caused by the major deformation induced by repeated indentations. The superficial recrystallization of the sample also tended to be more continuous for higher number of passes; micrographs of the penetration profiles of indentation in the samples rolled with high roughness rolls revealed that a sample rolled 24 times had not yet reached the steady surface topology. As a conclusion, in order to successfully form superficial nanograins, very low roughness rolls must be used as well as a small absolute reduction per pass, followed by annealing. These rolling conditions generate a continuous field of highly superficial deformations, which act as nucleation centers for nanograins during annealing.
KEYWORDS: Surface. Nanograins. Rolling. Rough rolls. Annealing.

1 INTRODUCTION

The development of the economy, with an annual increase of 3.7% on the global growth product since 2003, has generated an increasing demand for metals, which have risen in price, sometimes drastically; for example, the price of copper has increased by 409.5%. In that context, the international scientific community has made efforts to improve the mechanical and chemical performance of metals in order to optimize their use and widen their range of applications. In that sense, it is known that the presence of small grains favors the mechanical resistance of metallic materials. This phenomenon can be observed from the classic Hall–Petch equation, which indicates that smaller grain sizes produce higher yield strengths. This relationship has led to several investigations on refining the grain size of metallic materials. The methods used to refine the grain size to microscale and nanoscale regimes can be classified into three groups depending on the phases involved in the process: solid-state methods, solidification methods, and condensation/solidification methods. A number of studies have analyzed the deformation-recrystallization sequence of solid-state methods, a sequence which causes severe plastic deformation to the grain structure 3. This methodology has industrial limitations because of the size of the pieces and the high amounts of energy needed process the entire bulk structure instead of only its surface.

Other investigations have developed means of refining surface grains by inducing highly peripheral deformation and then recrystallizing the material; these deformation methods include sandblasting, shot-blasting, ultrasound pulses , wire-brushing and, more recently, high-speed waterjet deformation. For example, a previous report demonstrated the generation of a nanocrystalline surface layer on AISI 316 stainless steel by sandblasting with 0.75-mm alumina grains followed by annealing; this process refined the grains and increased hardness to a depth of 200-μm. Similar results have been obtained on AISI 304 stainless steel by sandblasting with 0.21–0.30-mm silica grains followed by annealing; this process produced 20-nm grains ; the presence of this surface layer considerably improved the steel's corrosion resistance and mechanical properties.

Another technique that has been used to obtain superficial nanograins is superficial deformation/recrystallization induced by wire brushing. In fact, a previous study demonstrated the generation of 20–300-nm superficial equiaxed grains on low-carbon steel alloys, austenitic stainless steel, commercial aluminum, Al-Mg, Al–4% Cu, pure Cu, Cu-Zn, and Pb-Sn; the authors of that study indicated that this technique can easily generate superficial nanostructures on any metallic alloy.

Additionally, several authors have reported the presence of nanocrystals in metallic surface layers after pin-on-disk tests performed on train rails or induced by friction. Nonetheless, none of these techniques are compatible with ongoing processes or for processing large surfaces, because they are slow and have low operative speed.

Because of these limitations, in this work the possibility of generating superficial nanostructures by other means is addressed. Specifically, cold rolling with rough rolls, thus simulating the superficial deformation processes occurring in sandblasting, could generate a dense, complex, high field of superficial deformations in a 316L stainless steel, and with a subsequent low-temperature annealing would induce the desired superficial nanostructures.

In effect, the application of a strong microcontinuous deformation field in a certain volume near the roll accumulates enough energy that new crystals can form at temperatures as low as 275°C. These new grains will be smaller than the original grains, given that a higher amount of energy can enter in the original network and that more nucleation centers are generated. Sandblasting and shot-blasting have produced positive results, but they cannot be used to treat large surfaces while maintaining proper dimensional control. The methodology proposed in this report simulates the deformation generated by these processes while allowing for better dimensional control and the possibility of treating larger surfaces.

2 EXPERIMENTAL DETAILS

A 316L austenitic stainless steel sheet with a nominal thickness h_0 of 5 mm, previously normalized at 900°C for 12 h, was considered as a raw material. To cold roll the sheet, was used a 7.5 kW Joliot two-high reversible rolling mill, equipped with rolls that were 200 mm wide and 127 mm in diameter. Based on the grain sizes of alumina and silica (between 0.21 and 0.75 mm) used for sandblasting samples of stainless steel in previous reports, three rolls with varying degrees of roughness were used in this work, between one half of the minimum to twice the maximum of the roughness considered by the cited references. The three rolls used are as follows: rolls with 0.17-mm and 0.33-mm average height surface grains (from ten measurements with standard deviation of 0.05 and 0.08 mm respectively), referred to as low-roughness rolls, and a roll with rhomboid-shaped base pyramids of 2.08-mm length, 1.04-mm width, and 1.5 -mm height on its surface, referred to as the high-roughness roll. The surface heights size of grains of the rough rolls were obtained by measuring it with a probe on a micrometer screw of 0.01 mm sensibility.

The 316L stainless steel normalized at 900°C was cold rolled first with the low-roughness rolls; the relative reduction was varied as well as the number of passes, up to 107. These variations were introduced in order to study the real effect on the generation of surface nanograins of the total reduction and that of repeated indentation induced by roll roughness. From the first set of results, obtained with low-roughness roll, it was deduced that the most important variable for generating new recrystallized grains was the number of passes; thus, when the high-roughness roll was used, the sheet was rolled in four different ways while keeping a fixed total reduction of 26%, reaching the final nominal thickness h_f of 3.7 mm but varying the number of passes and the absolute reduction per pass. Then, the cold-rolled samples were annealed at 275°C for 1 h. In the pattern samples (normalized) and those cold rolled and annealed, the Vickers microhardness (HV) - with a load of 30 Kg- using a Struers Duramin equipment was measured, and microstructures by optical microscopy were determined.

3 RESULTS

Figure 1 shows a typical micrograph of 316L stainless steel normalized at 900°C for 12 h and cooled in the furnace. The central zone of the sample shows 150-μm recrystallized grains; also, the formation of a fragile oxide layer with 50-μm grains was detected.

Figure 1. Micrograph of a 316L stainless steel sheet normalized at 900°C for 12 h.

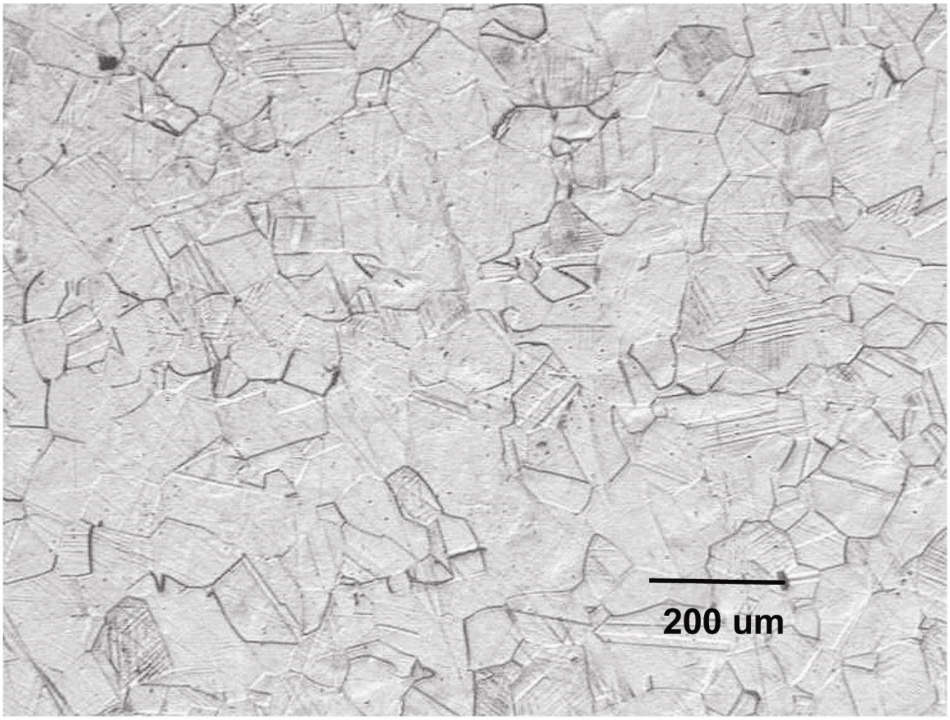

Table I shows the absolute reductions, numbers of passes, and characteristics of recrystallization obtained after annealing in the rolling assays with low-roughness rolls.

Table I. Characteristics of the assays made with low-roughness rolls.

Sample	Height grains (mm)	h_o (mm)	Number of passes	h_f (mm)	Results	Location
r18	0.33	4.94	18	4.69	Partial recryst.	surface
r12	0.33	4.92	12	4.46	No recryst.	
r26	0.33	4.94	26	4.73	Continuous.	surface
r7	0.17	4.81	7	4.64	No recryst.	

Sample	Height grains (mm)	h_o (mm)	Number of passes	h_f (mm)	Results	Location
r22	0.17	4.77	22	3.92	Partial recryst.	surface
r107	0.17	4.93	107	4.03	Continuous.	surface
r54	0.17	4.95	54	3.68	Continuous.	surface
r3	0.17	4.78	3	3.48	Partial recryst.	internal

In Table I and then in Table II, surface recrystallization refers to that from the surface to a 50-μm depth, while internal recrystallization refers to that from a 600- μm depth and below; partial recrystallization refers to that associated with zones of maximal deformation in the indentation marks or the planes of highest deformation. Also, in those tables the rolled samples were named r (number of pass) or R (number of pass) when low or high roughness rolls were used respectively.

Table I shows that continuous recrystallization on the surface is only achieved when the sample is rolled at least 26 times, independent of the total reduction. It is necessary to create a high and tangled density of deformations at the surface of the steel induced by the continuous indentation of the rough roll; these deformations will act as preferential nucleation sites during subsequent heating. Sticking friction is produced at the interface of the steel and roll as well as through some depth because of the indenter effect of the roll roughness, the latter of which increases with absolute reduction and the roughness itself; thus, it is deduced that global or bulk deformation does not affect surface recrystallization. In other words, the surface of the steel deforms mainly because of the indentation and not because of the deformation of the rolling itself.

Table II shows the absolute reductions, number of passes, and characteristics of recrystallization obtained after annealing in the rolling assays with high-roughness rolls.

Table II. Characteristics of the assays made with high-roughness rolls.

Sample	h_0 (mm)	Number of passes	h_f (mm)	Results	Location
R06	4.96	6	3.66	Partial recryst.	Int. – ext.
R10	4.96	10	3.79	Partial recryst.	Int. – ext.
R19	4.95	19	3.59	Partial recryst.	Int. – ext.
R24	4.96	24	3.62	Continuous	Int. – ext.

As shown in Table II, the assays with high-roughness rolls exhibited partial or continuous internal and superficial recrystallization after annealing at 275°C for 1 h, based on the number of passes and independent of the absolute reduction imposed. Figure 2 shows that samples rolled with 6 and 10 passes have certain sections on the surface with no new grains as well as other zones with smaller recrystallized grains of 10–15 µm. For the sample cold rolled with 24 passes, these small recrystallized grains appear over the entire surface, a behavior which highlights the cumulative effect of deformations by indentation based on the number of rolling passes.

Figure 2. Micrographs of the four different cold rolled samples annealed at 275°C for 1 h.

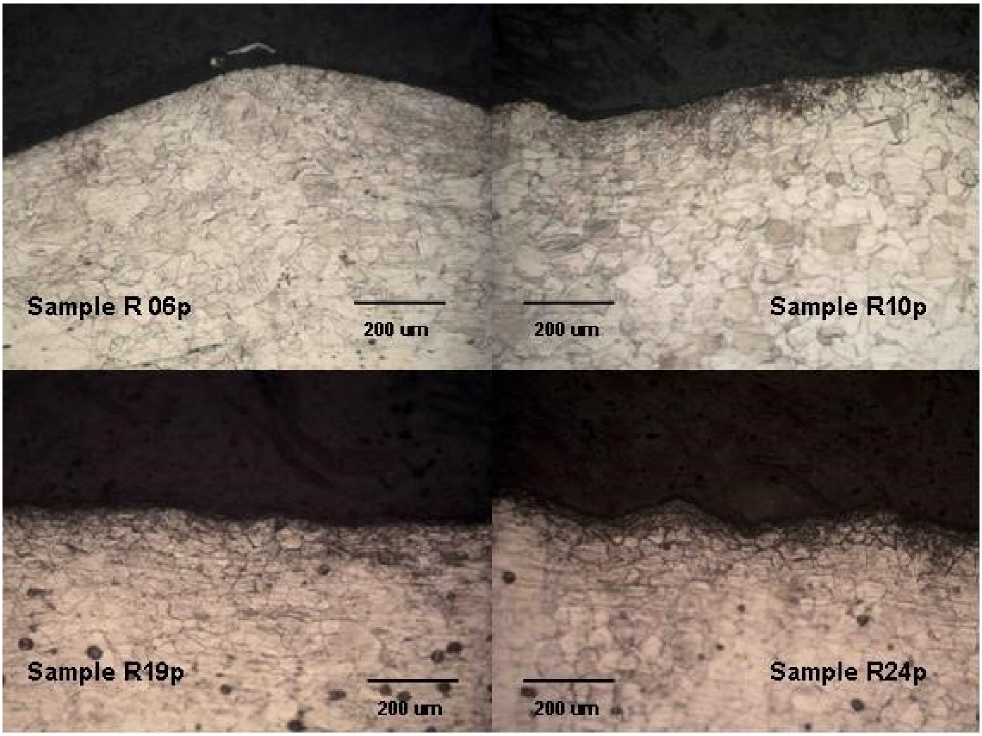

Figure 3 shows that preferential recrystallization with smaller (10–15 µm) grains can be observed from the surface. Zone 1 (to depth of 100 µm) is mostly affected by the indentation deformation caused by shear, which is imposed by the roughness of the roll. The recrystallized surface grains of 10–15 µm appear in this zone at a depth of 35–50 µm; these grains are considerably smaller than the remaining recrystallized grains in this sample. This behavior suggests a preferential indentation effect imposed by the roughness on this superficial deformation and the subsequent recrystallization. Zone 2 is located deeper in the sample; this zone contains larger recrystallized grains, which are produced by deformation from slip associated with the rolling itself and from some shear strain due to the effect of indentations that can reach such a depth. Zone

3, starting from a 600-μm depth, has recrystallization associated only with the rolling deformation from slip on bulk.

Figure 3: Micrograph of the R10 sample after rolling and annealing.

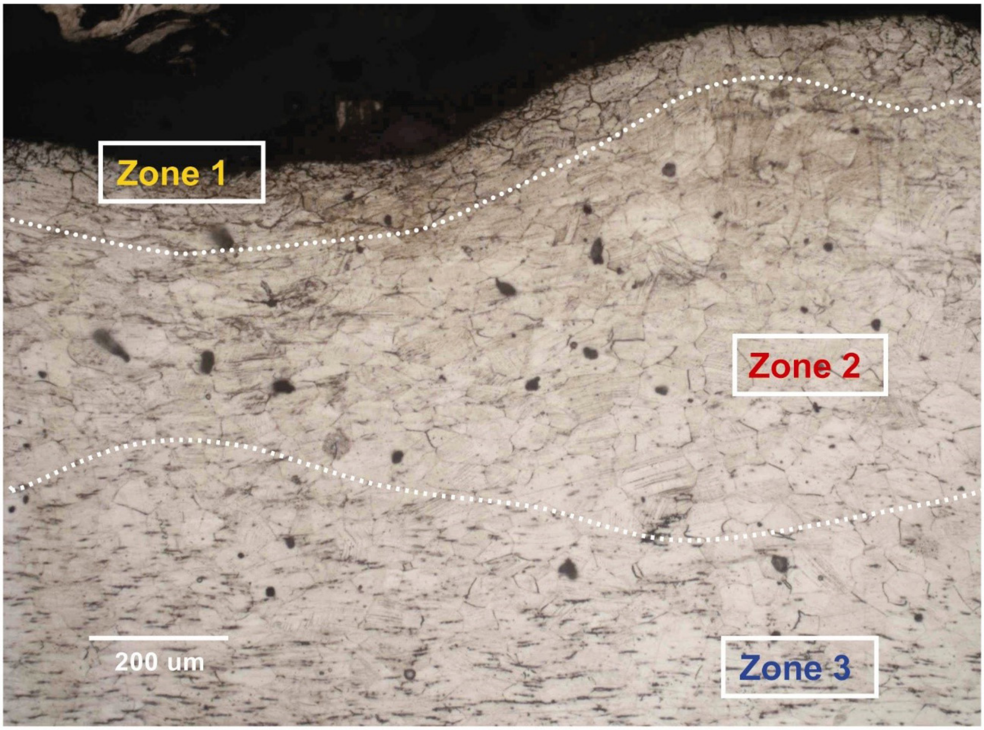

Figure 4 shows the microhardness profiles of two of the samples cold rolled with high-roughness rolls and then annealed; they are compared with those normalized at 900°C for 12 h and then sandblasted with granulometry sand of 0.21–0.30 mm for 20 min, followed by annealing at 275°C for 1 h with furnace cooling.

The hardnesses of the sandblasted and rolled samples at 50 μm from the surface are 240 and 210 HV, respectively. As previously mentioned, the grain size and hardness in this zone are associated only with the deformation caused by indentation. At greater depths, the hardness of the sandblasted sample decreases greatly to about 60 HV, the same as stainless steel annealed at 900°C. This phenomenon does not occur in the rolled stainless steel R06 and R24 in whose there is an increase of hardness to the deeper Zone 2 shown in Figure 3; this region shows a combination of the effects of the deformations by rolling and by indentation. From 600-μm depth, zone 3 of Figure 3, the hardness tends toward a stable value due to the only effect of the volume deformation by rolling.

Figure 4. Volumetric hardness's in samples that were cold-rolled or sandblasted and subsequently annealed.

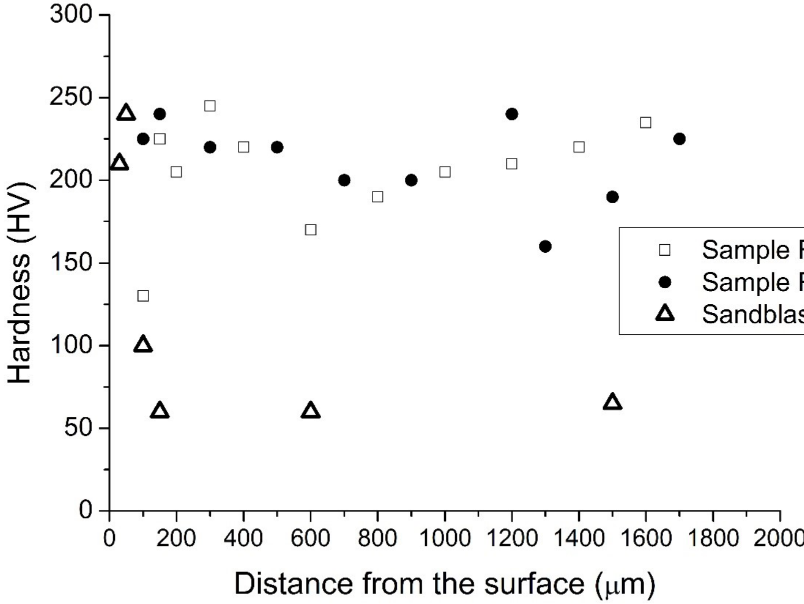

Figure 5 shows how the number of passes affects the indentation imposed in the sample cold rolled with high-roughness rolls.

Figure 5. Micrographs of the superficial topography of samples after 6, 11, 19 and 24 passes respectively from left to right, with high-roughness rolls.

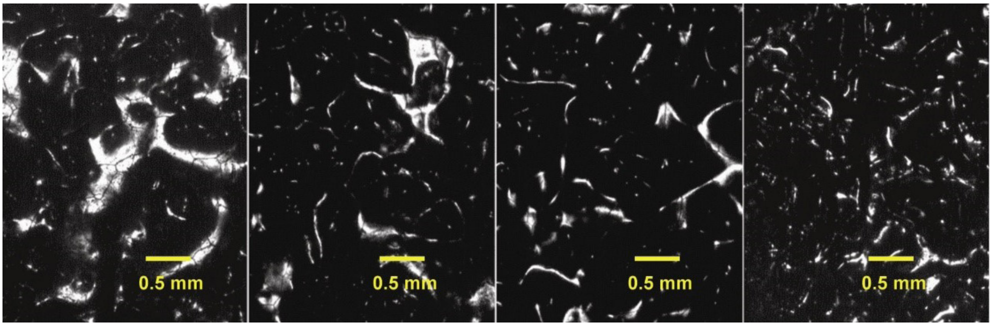

In each micrograph from Figure 5, the large white areas represent higher zones or plateaus from the material removed by indentation from the rough rolls. As the number of passes increases, these plateaus continue to interact with the roughness of the roll; this behavior tends to cause the surface of the steel to flatten, reducing the macroscopic effect of the indentation and diminishing the visibility of these plateaus in the micrographs. Nevertheless, the sample with 24 passes still exhibits visible white zones, although many fewer than the other samples. Studying the morphological evolution of the surface as the number of passes increases, as shown in Figure 6, a continuous increase of the density of concave regions and a decrease of the plateaus was found; thus, with respect to the studied roughness, the superficial deformation by indentation did not reach its steady topology conditions. This behavior coincides with the results of cold rolling with low-roughness rolls, as shown in Table I which both indicate the need of at least 26 passes to achieve a stable superficial imposition and, after annealing, continuous recrystallization of the surface.

4 CONCLUSION

The roughness of the roll imposes on the surface of the samples sticking friction and to avoid this surface adherence it is necessary to use rolls with lower roughness than those used in this work.

Cold rolling the sheet with rough rolls up to 24 passes did not produce a steady topology by indentation; wide plateaus visible on the surface, indicators of non-deformed material, progressively disappeared but did not do completely.

The industrial applicability of this process demands that the number of passes should be as low as possible, ideally between 5 and 10, when obtaining proper surface indentation. Thus, rolls with much lower superficial roughness than those used in this work should be considered; doing so will produce a much higher concentration of superficial points with high deformation, thus generating more nucleation centers during the annealing, producing more desirable superficial nanostructures.

The hardness at a depth of 50 μm achieved in the samples rolled with high roughness rolls is of the same order of that for the reference sandblasted sample. Nonetheless, the same recrystallization uniformity or grain size obtained from the sandblasted sample was not achieved. This result is caused by the differences in the complexity and homogeneity of the deformations imposed, a higher density of which can be obtained from sandblasting. Because of roughness of the rolls used, this effect was not reached in the samples of this report. A roll with lower roughness will cause the surface of the steel, over many rolling passes, to accumulate a tangle of indentation deformations, which is a necessary phenomenon not obtained in this work. Thus, only having a good hardness is not sufficient evidence of a structure with good conditions to generate nanograins after thermal treatment.

REFERENCES

Azushima, Severe plastic deformations (SPD) for Metals, *CIRP Ann.-Manuf. Techn.* 57, (2008): 716–735.

A. Gallegos, "Nuevas Técnicas de nanoestructuración superficial en un acero inoxidable 316L (New techniques for obtaining surface nanostructures on a 316L stainless steel)" (PhD diss., Universidad de Concepción, 2012).

C.T. Kwok, Corrosion characteristics of nanostructured layer on 316L stainless steel fabricated by cavitation- annealing, *Mater. Lett.* 60, (2006): 2419–2422.

H.A. Yun-wei, The wear and corrosion resistance of shot peened-nitrided 316L austenitic stainless steel, J. *Iron Steel Res. Int.* 16, (2009): 68–72.

Ministerio Economia y Finanzas Peru, marco macroeconomico trianual 2014-2016 (Economy and Finance Ministry of Peru, Triennial annual macro economy projection 2014-2016), 2013. http://www.bcrp.gob.pe/docs/Publicaciones/Programa-Economico/mmm-2014-2016-mayo.pdf. Accessed September 2013.

M. Multigner, Influence of the sandblasting on the subsurface microstructure of 316LVM stainless steel: Implications on the magnetic and mechanical properties, *Mat. Sci. Eng. C* 29(4), (2009): p. 1357–1360.

M. Sato, N. Tsuji, Y. Minamino, and Y. Koizumi, in High Performance structures and materials, *Technol. Adv. Mat.* 5(1–2), January-March (2004): 145–152.

N. Tsuji, Y. Saito, H. Utsunomiya, and S. Tanigawa, Ultra-fine grained bulk steel produced by accumulative roll- bonding (ARB) Process, *Scripta Mater.* 40(7), (1999): 795–800.

Rezaee, The influence of reversion annealing behavior on the formation of nanograined structure in AISI 201L austenitic stainless steel through martensite treatment, *Mater. Design* 32, (2011): 4437–4442.

S. Barriuso, Roughening of metallic biomaterial by abrasive less water jet penning characterization and viability, W*ear* 270, (2011): 634–639.

S. Emgea, D. Karthikeyanb, and A. Rigney, Effect of the boronzing on the dry wear behaviour of DC53/0.45 mass % C steel, *Wear* 267, (2009): 562–567.

X.H. Chen, Tensile properties of a nanocrystalline 316L austenite stainless steel, *Scripta Mater.* 52, (2005): 1039–1044.

X.Y. Wang, Mechanical and electrochemical behavior of nanocrystalline surface of 304 stainless steel, *Electrochim. Acta* 47, (2002): 3939–3947.

X.Y. Wang, Mechanical, electrochemical and tribological properties of nanocrystalline surface of 304 stainless steel, *Wear* 255, (2003): 836–845.

X.Y. Wang, Mechanical, electrochemical and tribological properties of nanocrystalline surface of brass produced by sandblasting and annealing, *Surf. Coat. Technol.* 167, (2003): 188–196.

ABOUT THE ORGANIZER

MARCOS AUGUSTO DE LIMA NOBRE: Assistant Professor and Researcher (2006 - present), with citation name M. A. L. Nobre, at the São Paulo State University (UNESP), School of Science and Technology, Department of Physics, campus at Presidente Prudente-SP. Head and Founder (2002) of the Laboratory of Functional Composites and Ceramics (LaCCeF acronym in Portuguese, the native idiom), Lab certified by PROPE-UNESP/National Council for Scientific and Technological Development/CNPq*. Grants from National Council for Scientific and Technological Development (CNPq), 2020-2023, 2019-2021 and 2010-2012. Granted with Young-Researcher scholarship by the São Paulo Research Foundation, FAPESP (São Paulo, São Paulo) (2002 - Summer of 2005). Postdoctoral fellow at the Polytechnic School of the University of Sao Paulo (POLI USP-SP) Metallurgy and Materials Science Department with FAPESP Scholarship (1999-summer of 2000). PhD in Science, CAPES Scholarship (Physical Chemistry 1999) by the Chemistry Department, UFSCar-SP. Master in Chemistry CNPq scholarship (Physical Chemistry 1995) by the Chemistry Department, UFSCar-SP. Licentiate degree (4-year of study) in Physics (1993) CNPq and CNPq-Rhae scholarships by the Physics Department, UFSCar-SP. Associate Editor of the Micro & Nano Letters - IET 2019-2020. Associate Editor of the Micro & Nano Letters-Wiley, 2020 - present. Ethycal Editor of the Applied Mathematics Science (Reuse) m-Hikari and Modern Research in Catalysis, Irvine-CA, USA (2017- date). Editorial board member of the Artemis Editora, Brazil. Nowadays, have 02 patents. Has published 80 papers at 39 different indexed Journals of renowned Editors. In May/25/2021, has been cited 1379 times, at 76 papers (47 with citations), in according to the ResearchID actual Publons base having an H-index equal to 23. Academic Google score: H = 28, i10 = 45 and 2338 citations. Reviewer of more than three dozen of journals. Have more than 580 communications and presentation in National and International Congress and Symposiums, from these 150 has been published as Conference Paper. Author or co-author of 20 Chapters of book approaching Scientific Divulgation, Teaching of Physic and Chemistry for teachers actuating in the graduating degree. For this, the Nanoscience and Nanotechnology have been the first strategy. Received tens of National and International Awards, Honorable mentions and distinction mentions, as well as titles. Research skills: Materials Science, Advanced Ceramic Processing, Linear and Non-linear Advanced Dielectrics Materials, Solid state chemistry, Impedance spectroscopy of solids and fluids, Structural Characterization via Mid infrared Spectroscopy with Fast-Fourier-Transformed of solid and fluids, Structural and non-structural Phase Transitions in Semiconductor Ferroelectrics. Also, Molecular Interactions in Functional Fluids as biofuels and its blends, probed via mid infrared Spectroscopy. Research interests: New Functional Materials as amorphous composite based on carbon/nanoparticles and Semiconductor Ferroelectrics. Member of the Program of Post-Graduation in Chemistry at UNESP - Campus of São José do Rio Preto, IBILCE UNESP – SP, Brazil.

INDEX

A

Adsorbente 172, 173, 179, 180

Alumínio 182, 183, 184, 186, 187, 189, 190, 191, 192, 193, 198, 200, 204, 205, 206, 208, 209, 210

Annealing 1, 2, 4, 5, 7, 9, 10, 227

Arsénico 172, 173, 174, 178, 179, 180, 181

AuNR dimer 12, 14, 16, 17, 18, 19

B

Biodiesel 162, 164, 165, 168, 169, 171

Blends 162, 168, 169, 170, 171

Bulk sensitivity 12, 14, 15, 16, 17, 18, 19, 73

C

Carboxymethylchitosan 125, 127, 128, 129, 132, 133, 136

Celulose 228, 229, 230, 231, 232, 233

Chemical composition of SS surface 109

Clay 125, 127, 128, 130, 131, 133, 136, 137

Comparison among Silica and reuse of waste 77

COMSOL 14, 15, 68

Conductive tubes 92, 93, 94, 95, 100, 102, 104, 106

Confined water 39, 40, 41, 42, 52, 55, 58, 59, 60, 61, 63, 65

D

DFT 21, 23, 35, 36, 49, 50, 63

Diesel 162, 163, 164, 165, 168, 169, 171

DSSC 213, 214, 217

E

Efluente 172, 173

Evolutionary strategies 151, 156

F

FEM 14, 68

Figure of merit 11, 12, 14, 15, 16, 17, 67, 68, 72, 73, 74

Filmes finos 205, 212, 213
Filter 125, 126, 127, 128, 131, 132, 134, 135, 136, 137
Fits on Mössbauer spectra 151
FoM 15, 16, 17, 18, 19, 68, 74

G

Graphite nanostructures 162

K

$KSr_2Nb_5O_{15}$ ceramic 138, 139, 141, 144, 146

M

Magnetita nanoestructurada 172, 173
Metalurgia do pó 182, 186, 191, 192
Métodos químicos 198, 201, 205
Micro and nano silica 76, 77, 78, 79, 84, 90

N

Nanocomposite 36, 37, 91, 125, 126, 127, 128, 132, 133, 134, 135, 136, 137, 161, 182, 183, 194, 195, 196, 198, 211
Nanocompósitos 182, 183, 185, 186, 193
Nanocristais 228, 229, 230, 232, 233
Nanoestruturas 182, 198, 200, 201, 202, 206, 210, 213, 217, 218, 219, 222, 223, 224, 226
Nanograins 1, 2, 3, 9, 138
Nanolithography 39, 40, 41, 42, 45, 50, 62, 64, 66
Nanopartículas 151, 180, 212, 224, 228, 229, 231
Nanostructures 2, 9, 12, 13, 14, 15, 17, 19, 21, 22, 23, 25, 38, 61, 68, 69, 70, 71, 72, 74, 138, 162, 170, 211, 213, 226, 227
Nanostructures surface 21, 22, 23
Nanotechnology 12, 20, 62, 66, 102, 106, 126, 138, 162, 183, 195, 213, 226
Nanotecnologia 182, 212
$NiFe_2O_4$ nanoparticles 150, 151, 153

O

Oxidation 39, 40, 41, 42, 53, 55, 59, 64, 65, 91, 109, 117, 118, 121
Óxido de grafeno reduzido 182, 183, 186

Óxido de zinco 197, 213

P

Papel reciclado 228, 229, 232, 233
Perfectly matched layer 11, 12, 15, 68, 69
PIII in magnetic field 109
Plasma immersion ion implantation 92, 93, 94, 107, 108, 109, 122, 123, 124

R

RI 15, 16, 67, 68, 72, 73
Rice husk Silica 77
Rolling 1, 2, 3, 4, 5, 6, 7, 9
Rough rolls 1, 2, 3, 8, 9

S

SILAR 198, 200, 201, 204, 205, 206, 210, 212, 213, 216, 217, 218, 219, 220, 221, 222, 223, 224, 226
Silica Morphology 77, 83
Silver nanoparticles 74, 125, 127, 128, 129, 130, 132, 133, 136, 137
Supercapacitores 197, 198, 199, 200, 202, 209, 210
Surface 1, 2, 3, 4, 5, 6, 7, 8, 9, 10, 11, 12, 14, 19, 20, 21, 22, 23, 24, 27, 28, 29, 30, 31, 33, 34, 35, 36, 37, 38, 39, 40, 41, 42, 44, 45, 50, 52, 53, 54, 55, 57, 58, 59, 60, 63, 64, 65, 66, 68, 69, 70, 75, 77, 79, 80, 81, 82, 84, 85, 88, 91, 92, 93, 94, 95, 96, 98, 99, 100, 102, 103, 104, 105, 106, 107, 108, 109, 110, 111, 112, 113, 114, 116, 117, 118, 119, 121, 122, 129, 152, 160, 161, 173, 211, 213, 226, 227
Surface modification 37, 38, 92, 93, 106, 109, 110

U

Ultrananocrystalline Diamond Films 93, 108

V

Viscosity 89, 162, 163, 165, 166, 167, 168, 169, 170, 171

X

X-ray photoelectron spectroscopy 42, 92, 96, 103, 108, 109, 111, 123

Z

ZnO 21, 22, 23, 24, 25, 26, 27, 28, 29, 30, 31, 32, 33, 34, 35, 36, 37, 38, 197, 198, 199, 200, 201, 202, 204, 205, 206, 207, 208, 209, 210, 211, 212, 213, 214, 215, 217, 218, 219, 220, 221, 222, 223, 224, 225, 226, 227

ZnO nanocrystals 21, 23, 25, 35

EDITORA
ARTEMIS